

Shear Strength Evaluation for RC Shear Walls With Multi-Openings Based on FEM Analysis

Masato SAKURAI & Hiroshi KURAMOTO

Osaka University, Japan

Tomoya MATSUI

Toyohashi University of Technology, Japan



SUMMARY:

Two dimensional non-linear finite element analyses for reinforced concrete shear walls with two openings were conducted to investigate the shear force contributions and internal stress transferring mechanisms. Parametrical analyses were also conducted for the shear walls with several opening layouts. The analytical results showed that compressive diagonal struts transferring shear forces were formed in each wall element and their shape depended on the wall panel length, regardless of opening layouts and loading directions. Then, it was clarified that the contribution to shear force of each wall element increased with the increase of the wall panel length, and also that the boundary column with tensile forces contributed only about 10% or less of the maximum shear force. On the basis of the analytical results, a simplified shear resistant model for shear walls with multi-openings was proposed. It was clarified that the shear strength of RC shear walls with multi-openings can be evaluated by the proposed model.

Keywords: RC shear walls with openings, Multi-openings, Shear strength, FE analysis

1. INTRODUCTION

In Japan, the shear strength of reinforced concrete (RC) shear walls with openings is estimated by multiplying the strength of the shear walls without opening by a reduction factor based the opening details. However, according to the existing experimental results and the actual damages under real seismic forces, the behaviour of RC shear walls with multi-openings is very complex. Especially, the shear strength, hysteresis characteristics, failure mode and deformation capacity of RC shear walls with several opening layouts are more significantly influenced than specified by the simplified methods in the AIJ standard for RC buildings (2010). Moreover, little quantitative evaluation for the seismic performance of the shear walls with multi-openings has been done so far.

The main objective of this study is to propose the quantitative evaluation for RC shear walls with multi-openings. In this paper, two dimensional non-linear finite element method (FEM) analyses for the shear walls with multi-openings were conducted to investigate contributions each shear wall element to shear force and internal stress transferring mechanisms. Parametrical analyses were also conducted for the shear walls with several opening layouts. On the basis of analytical results, a simplified shear resistant model for the shear walls with multi-openings was proposed.

2. FEM PARAMETRICAL ANALYSIS

2.1. Analytical Models

Parametrical analyses were conducted for the RC shear walls with several opening layouts. Details of the configuration of analytical models are shown in Fig.2.1. Specifications of sections and mechanical properties of materials used in the analysis are listed in Tables.2.1 and 2.2.

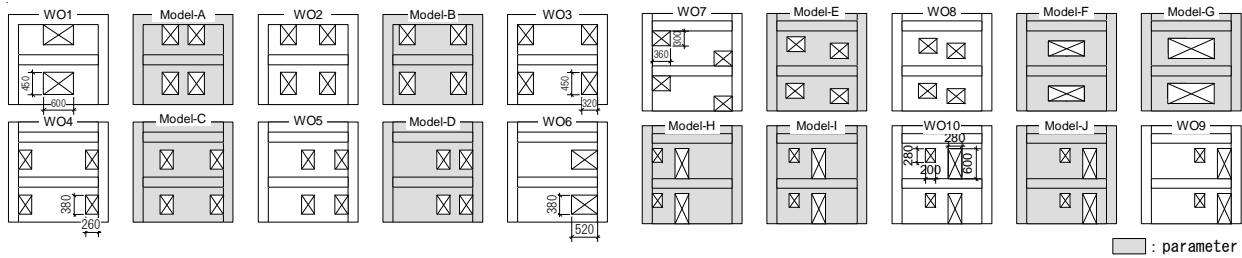


Figure 2.1. Analytical models

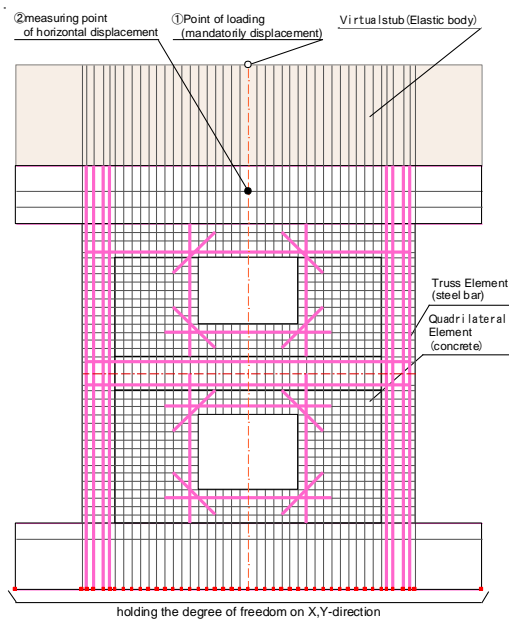


Figure 2.2. FEM mesh (Specimen WO1)

Table 2.1. Specification of section

	WO1~WO3 Model-A,Model-B	WO4~WO6 Model-C,Model-D	WO7,WO8 Model-E~Model-G	WO9,WO10 Model-H~Model-J
story height	1000(1st) 800(2nd)		800	
column	B × D 200 × 200			
	Longitudinal bar 12-D13 ($p_v=3.8\%$)			
	Tie 2-D6@60 ($p_v=0.53\%$)			
	Sub-tie 2-D@120 ($p_v=0.27\%$)			
beam	B × D 150 × 200(1st) 200 × 200(2nd)			
	Longitudinal bar 4-D10 ($p_v=0.54\%$)			
	Stirrup 2-D6@100 ($p_v=0.42\%$)			
	Thickness 80			
wall panel	Longitudinal bar D6@100zigzag ($p_v=0.4\%$)			
	Transverse bar D6@100zigzag ($p_v=0.4\%$)			
	Bar around opening D10 (longitudinal, horizontal, diagonal)		D10(longitudinal, horizontal)	

Table 2.2. Properties of materials in analysis

	WO1~WO3 Model-A,Model-B	WO4~WO6 Model-C,Model-D	WO7,WO8 Model-E~Model-G	WO9,WO10 Model-H~Model-J	
Concrete	σ_B (N/mm ²) 30				
	σ_t (N/mm ²) 0.91(Column·Beam)		0.45(Wall panel)		
	E_s (kN/mm ²) 12.5				
	ϵ_{sp} (μ) 4000				
	Steel bar	σ_y (N/mm ²)	D6	336	338
D10			327	348	344
D13			442	405	456
E_s (kN/mm ²)		D6	221	187	148
		D10	153	190	202
		D13	173	185	196

In the previous studies by the authors, static loading tests on RC shear walls with openings were carried out to investigate the influence of different number and arrangement of the openings (Sakurai et al. 2008 and Sakurai et al. 2010). Test specimens were designed to simulate the lower 2 stories of multi-story shear wall in medium-rise RC buildings and scaled to one third of the prototype wall. The variables investigated were the number and layout of the openings.

The analytical models were designed based on specimens in those tests. In the analysis, a total of 20 RC shear walls were analysed including 10 specimens tested by the authors (Specimens WO1 to WO10: Sakurai et al. 2009 and Sakurai et al. 2010) and 10 analytical models (Model-A to Model-J) to interpolate the test parameters. The equivalent perimeter ratio of opening for Specimens WO4 to WO6, Model-C, Model-D were equal to almost 0.35, while those for other specimens were equal to almost 0.4.

2.2. Analytical Method

The finite element mesh layout for Specimen WO1 is shown in Fig.2.2. A quadrilateral plane stress element was used for concrete. Reinforcing bars in the wall panels and transverse reinforcements of boundary columns and beams are substituted by equivalent layers with stiffness in the bar direction and superposed on the quadrilateral elements. Longitudinal reinforcing bars in boundary columns and beams were modeled by truss elements. Line elements were used between truss elements and quadrilateral elements to consider the bond slip behavior.

Each node at the end of the lower stub had pin support to restrain vertical and lateral displacement. The elements between the loading point prescribed shear-span ratio and the top end of upper stub were

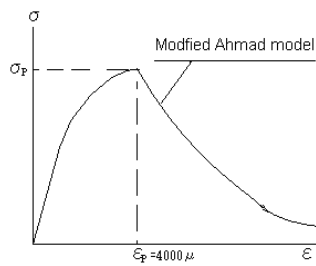


Figure 2.3. Stress – strain relationships

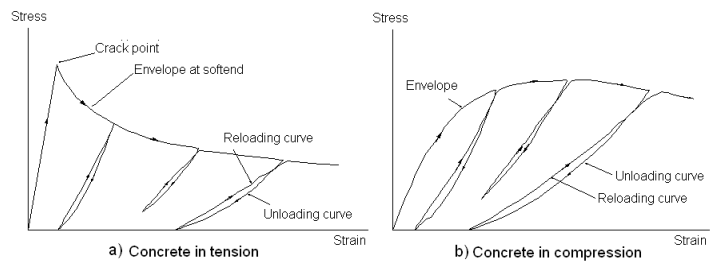


Figure 2.4. Reversal loading model of concrete in tension/compression

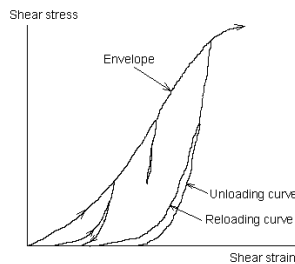


Figure 2.5. Reversal loading model of concrete shear along crack direction

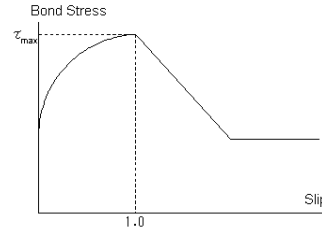


Figure 2.6. Bond stress– slip relationships

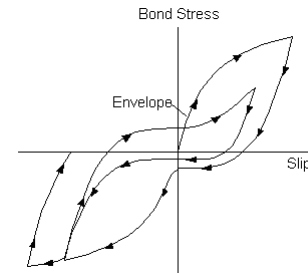


Figure 2.7. Reversal loading model of bond behavior

defined as an elastic body, which is a virtual stub. A node at the top of the virtual stub was subjected to lateral displacement reversals with applying a constant initial axial force. The FEM non-linear analysis software “FINAL” was used in this analysis (ITOCHU Techno-Solutions Corporation 2004).

2.3. Constitutive Laws of Materials

Concrete is idealized using the orthotropic model based on the strain concept. The smeared crack model for concrete elements was determined non-orthotropically crack model considered that it is able to represent multi-directional cracking (Naganuma et al. 2001). As for the stress-strain relationships of concrete, a modified Ahmad model was adopted for the stress-strain curve as shown in Fig.2.3.. Kupher-Gerstle’s criterion (1973) was applied for failure in biaxial compression and in tension-compression. Degradation of compressive strength and strain after cracking were incorporated. The compressive reduction factor was defined as a function of uniaxial compressive strength of concrete and acting normal stresses along reinforcing directions modeled on basis of RC panel tests by Naganuma (1991). In the stress - strain relationship under stress reversals, because of unloading and reloading response of concrete is not clear, unloading and reloading curves were represented using quadratic equations in compression and tension as shown in Fig.2.4 (Naganuma et al. 2000). In the tensile zone, the tension stiffening envelope after cracking determined as a function of the compressive stress and reinforcement ratio proposed by Yamaguchi and Naganuma (1990). The hysterical rule on the shear stress - shear strain relationship was modeled as shown in Fig.2.5. Shear transferring action is expressed by the average shear stress-shear strain relationship along the crack direction. The shear stress - shear strain envelope was determined as a function of the concrete strength, the amount of reinforcing steel crossing the cracks, and tensile strain perpendicular to the crack direction (Naganuma 1991). The bond stresses between reinforcing bars and concrete versus slip deformation relationships are shown in Fig.2.6. The maximum bond stress of concrete calculated by the AIJ design standard for RC buildings based on inelastic displacement concept (1999) and the sliding at the maximum bond stress was assumed to be 1.0mm. The reversal loading model of bond behavior was represented by the modified Elmsorsi model as shown in Fig.2.7 (Naganuma et al. 2004).

The material model of reinforcing bars was a plasticity model, which is the Von Mises model failure surface with associated plastic rule. The stress-strain curve of the reinforcing bars under stress reversal was idealized by Ciampi’s model (1982), and the isotropic hardening rule was adopted as the hysterical model.

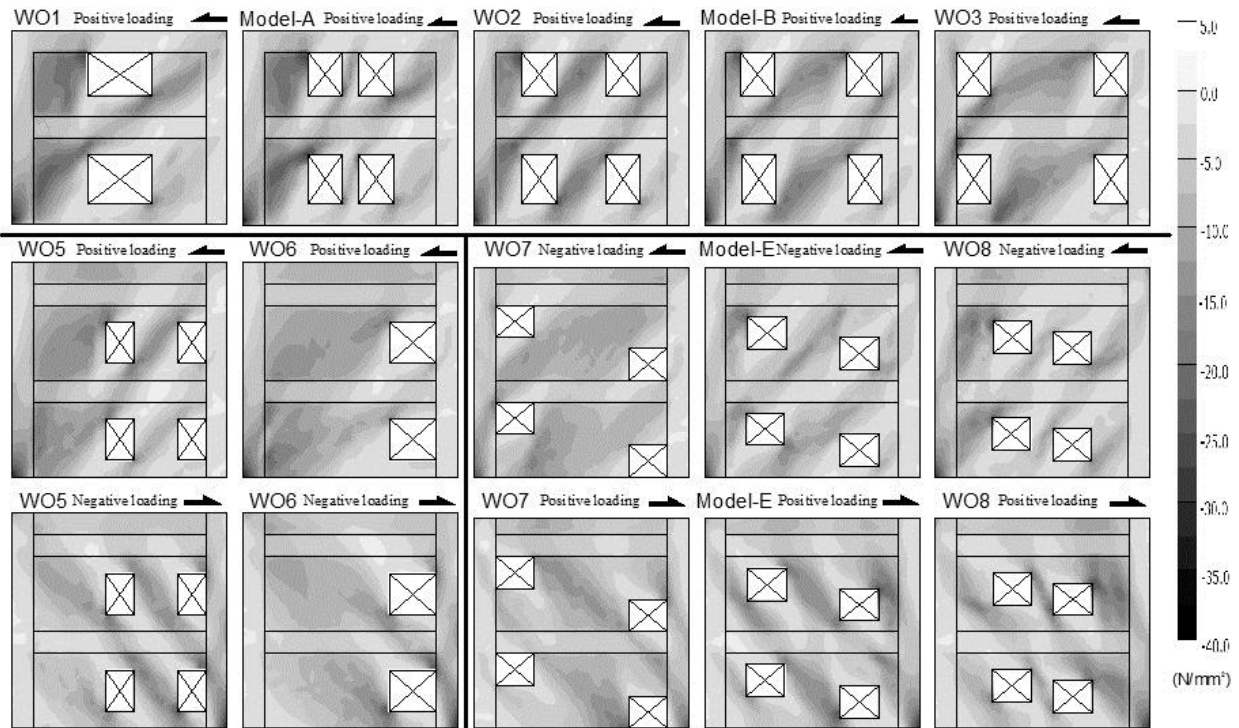


Figure 3.1. Principal compressive stress distributions of concrete elements ($R=1/200\text{rad.}$)

3. ANALYTICAL RESULTS

3.1. Internal Stress Transmission

The principal compressive stress distributions of concrete elements at the drift angle R of $1/200\text{rad.}$ for each specimen are shown in Fig.3.1. In Specimens WO1 to WO3, Model-A and Model-B which have symmetrically arranged openings, the analytical results have the same tendency either in the positive loadings and the negative loadings. Therefore, the results are shown only in the positive loadings.

In Specimen WO1 with one opening by floor at the center of wall panel, compressive struts were formed diagonally in each wing wall. In Model-A where two openings are located at a relatively close distance from center, the struts were formed in the central panel as well as the wing wall. In Specimen WO2 and Model-B which have smaller depth of the wing walls, the struts in the wing wall become narrow and with steeper angles than those of Specimen WO1. It was shown that compressive diagonal struts were formed in each wall element and the shape depended on the wall panel length. On the other hand, in Specimens WO5 and WO6 which have eccentric openings, the angles and widths of the struts were similar tendency regardless difference of the loading directions.

However, in Specimens WO7, WO8 and Model-E which have diagonally arranged openings, the struts in central walls were different from depending on the loading directions. For example, in the central panel of Specimen WO7 in the positive loading, the strut was formed between two openings, while in the negative loading, the struts were roughly transferred by two paths. One was a strut formed from top of the wall panel in the second story to the bottom of the central panel in the first story, and the another was a strut formed from top of the tensile column to bottom of central panel.

3.2. Contribution to Shear Force

The contribution to shear force in columns, wing walls and central panels at the first story at R of $1/200\text{ rad.}$ are shown in Figs.3.2 and 3.3 in order to grasp quantitatively the effect of the arrangement and the number of the openings on the shear stress transmission. The contribution to shear force by the wing walls, the central wall panels and the boundary columns were the sum of each quadrilateral element at the height given by dotted line in Figs 3.2 and 3.3. In Specimens WO1 to WO3, Model-A and Model-B which have symmetrically arranged openings, the analytical results have the same

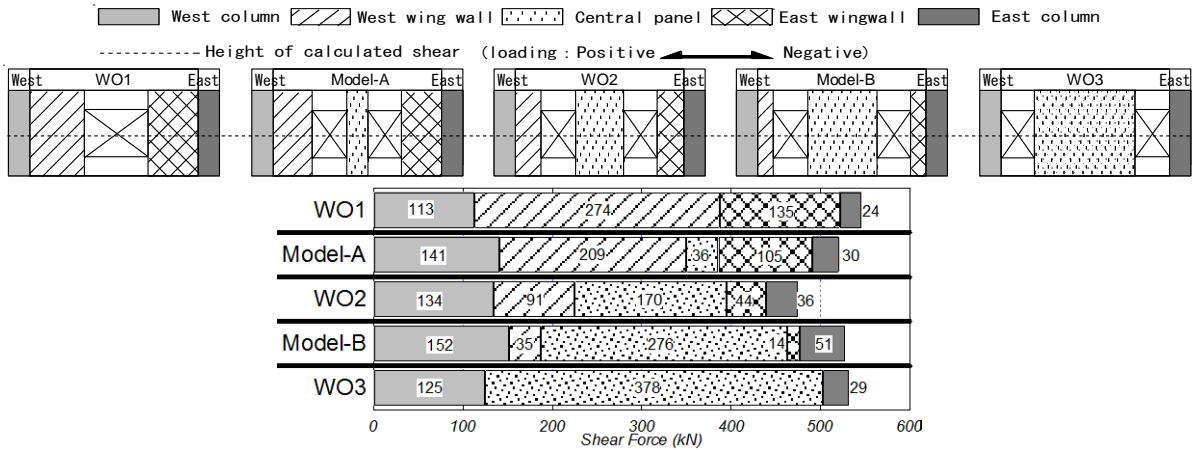


Figure 3.2. Contribution to shear force by each part (1st story, WO1~WO3, Model-A, Model-B)

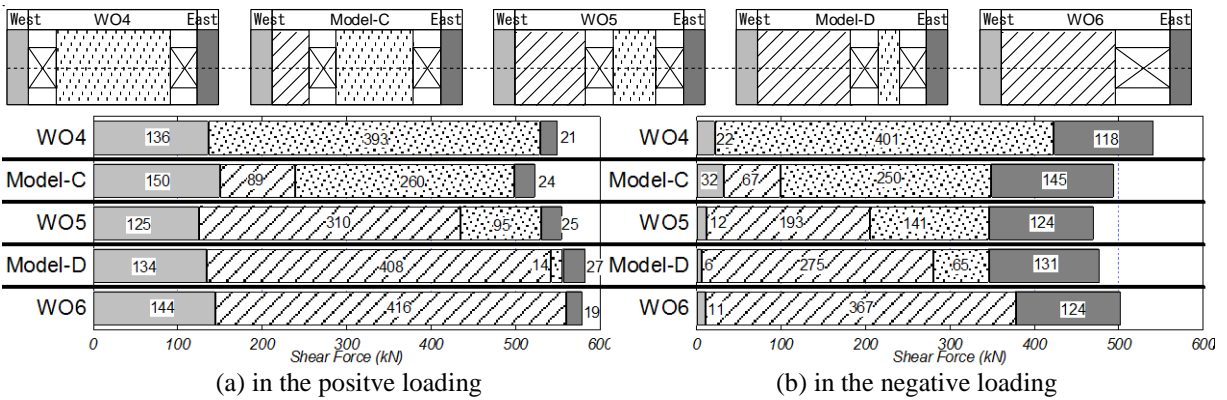


Figure 3.3. Contribution to shear force by each part (1st story, WO4~WO6, Model-C, Model-D)

tendency either in the positive loadings and the negative loadings. Therefore, the results in Fig.3.2 are only in the positive loadings.

The wing wall with compressive forces in Specimen WO1 contributed shear force of 274kN, while those in Model-B had only 35kN. Then, the contribution to shear force by the wing wall with tensile forces in Specimen WO1 was 135kN, while the observed in Model-A was 36kN. Thus, it became clear that the contribution to shear force by the wing walls decreased with the decrease of the depth of wall. The contribution to shear force by central wall panels was 36kN for Model-A and 368kN for Specimen WO3. Therefore, the contribution to shear force increased as increasing the depths of central panels. It was shown that the contribution to shear force by the wing walls, the central wall panels and the boundary columns varied with the variation of their depths. On the other hand, the boundary column with axial compression in each specimen contributed about 111 to 150kN, which was almost 30% of total shear force, while those with tensile force contributed about 6 to 32kN, which represents only 10% or less of total shear force.

4. SHEAR STRENGTH ESTIMATION OF RC SHEAR WALL

4.1. Shear Transmission Model

According to the analytical results, a simplified shear estimation for RC shear walls with multi-openings is proposed. As shown in Chapter 3, it becomes clear that the diagonal strut is formed depending on the depth of wall panels and columns regardless of opening layouts and loading directions. The test results showed that the shear strength deteriorations were observed when the walls adjacent to the opening failed in compression after reaching the maximum strength (Sakurai et al. 2008 and Sakurai et al. 2010). Thus, it is considered that a shear resisting mechanism is formed in the boundary columns, the wing walls and the central wall panels as shown in Fig.4.1. Namely, on the

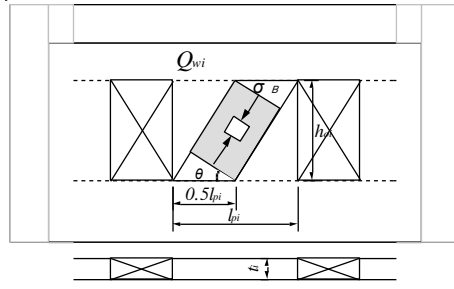


Figure 4.1. Proposed shear resisting model in wall panels

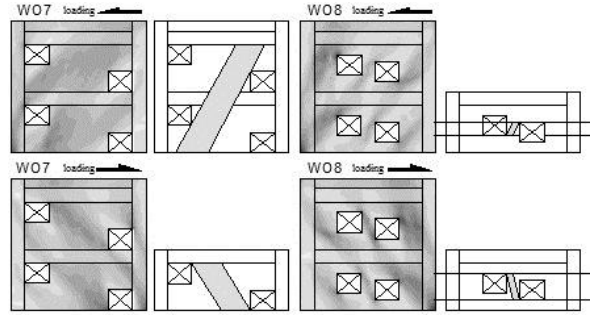


Figure 4.2. Assumption of strut in diagonal openings

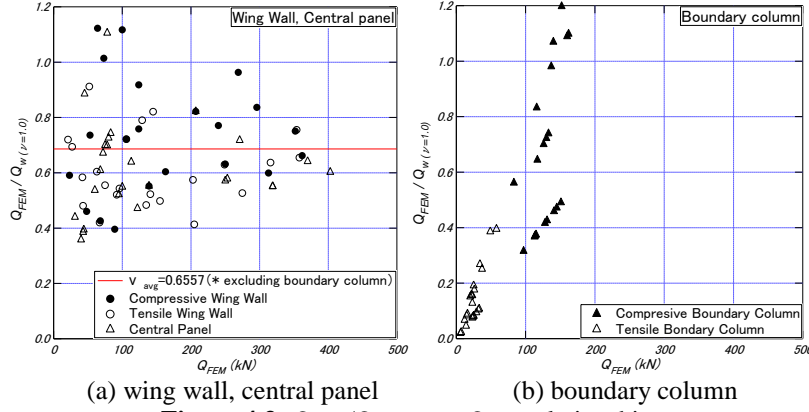


Figure 4.3. $Q_{FEM}/Q_{W(v=1.0)} - Q_{FEM}$ relationships

area between the openings, with a length of l_{pi} and opening height h_{pi} , it is assumed that a strut with a depth of $0.5l_{pi}$ is formed. Thus, the shear strength Q_w can be defined as shown in Eqn.4.1.

$$Q_w = v\sigma_B \cdot \cos\theta_i \cdot \sin\theta_i \cdot 0.5l_{pi} \cdot t_i \quad (4.1)$$

- where v : effective factor for compressive strength of concrete
 σ_B : compressive concrete strength (N/mm^2)
 θ_i : the angle of strut at wall panel
 l : wall panel depth (mm)
 t_i : wall panel width (mm)

As described in Chapter 3, in shear walls which have diagonally arranged openings such as Specimen WO7 and WO8, different struts are formed with the difference of the loading directions. Then, the angle of struts is assumed depending on the loading direction as shown in Fig.4.2.

The contributed shear strengths by Eqn.4.1 considering the boundary columns, wing walls and central panels are plotted in Fig.4.3. In the figure, the vertical axis shows the ratios of the contributed shear by wing wall, central panel and boundary column evaluated by FEM analysis, Q_{FEM} , to those calculated by Eqn.4.1 with the effective factor for compressive strength of concrete v of 1.0, $Q_{w(v=1.0)}$, while horizontal axis is Q_{FEM} .

As shown in Fig.4.3(a), average values of $Q_{FEM}/Q_{w(v=1.0)}$ at the wing walls and the central panels were varied around 0.65. On the other hand, the calculated results at boundary columns in tension overestimated the contributions to shear force given by FEM analysis, while those at boundary columns in compression are underestimated. As described above, assuming v of 0.65, the shear strength given by Eqn.4.1 in central panels and wing walls were evaluated roughly, while those in boundary columns varied widely.

4.2. Assumption of Boundary Columns

As described in Section 4.1, it is difficult to evaluate the contributed shear of boundary column by

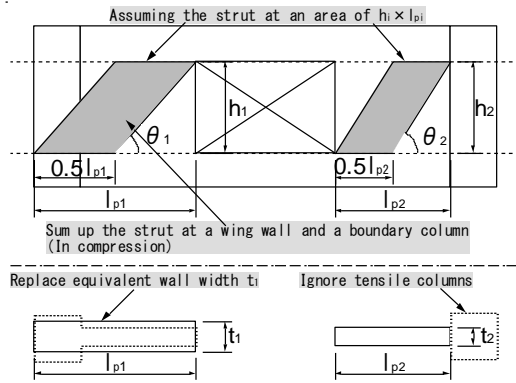


Figure 4.4. Assumption of boundary columns

Table 4.1. Parameters

Compressive concrete Strength σ_B (N/mm ²)	15, 20, 25, 30, 35, 40, 45, 50
Shear Span Ratio M/QD	0.6, 0.8, 1.0, 1.2, 1.4, 1.6, 1.8, 2.0
Wall Bar Ratio ρ_s (%)	0.2, 0.3, 0.4, 0.5, 0.6, 0.7, 0.8, 0.9, 1.0, 1.5, 2.0
Axial Force Ratio $N/bD\sigma_B$	0.05, 0.1, 0.15, 0.2, 0.25, 0.3

Eqn.4.1. Therefore, a simplified method in which the boundary columns and the wing walls work one body was adopted to calculate the shear strength.

As shown in Figs.3.2 and 3.3, in tensile boundary columns, the strut is very small. Then, their contribution to shear force for each specimen is about 10% or less of total shear force. Therefore, it was assumed that the shear force in tensile boundary columns can be ignored in the proposed models. On the other hand, the contribution to shear force in the compressive wing walls increased with the increase of the depth of its wing walls, while those in the compressive boundary columns represent about 30% of total shear force, regardless the depth of the wing walls. For simplified calculation, the struts in the boundary columns and the wing walls in compression are estimated collectively. Namely, in the wing walls and the boundary columns in compression, the width of the wall panel and the column were replaced by an equivalent wall width. Thus, it was assumed that a strut is formed at area of the wall depth which combined the wing wall and the boundary column, l_{p1} , and opening height, h_1 , as shown in Fig.4.4.

4.3. Examination of Effective Factor for Compressive Strength of Concrete

In the previous section a simplified model for the RC shear walls with openings which applied the struts in wall panels was proposed. However, it is expected that the variation of parameters such as shear span ratio, axial force ratio and wall steel ratio have influence on the shear strength of RC shear walls with openings. In the following section, the parametrical study for influencing parameters based on FEM analysis were carried out, to clarify the effects of compressive concrete strength, shear span ratio, axial force ratio and wall bar ratio of RC shear walls on the shear strength of RC shear walls with openings. Thus, on the basis of these results, the effective factor for compressive strength of concrete v in the proposed model was assumed as a function of these influencing parameters.

4.3.1. Parametrical Study for Influencing Parameters

Parametrical study for compressive concrete strength, shear span ratio, axial force ratio and wall steel bar ratio of RC shear walls was carried out, to investigate the effect of the influencing parameters of RC shear walls on their shear strengths. Intended parametrical models were Specimens WO1 to WO8 for which concrete cylinder strength was 30N/mm², shear span ratio was 1.30, axial force ratio was 0.2 and wall steel bar ratio was 0.4%. Additional models were varied influencing factors as listed in Table.4.1. Analytical methods and constitutive laws of materials were used the same as described in Chapter. 2.

4.3.2. Analytical Results

The calculated shear strengths by the parametrical studies, Q_p - compressive concrete strength relationships, Q_p - shear span ratio relationships, Q_p - axial force ratio relationships and Q_p - wall steel bar ratio relationships for Specimen WO1 are shown in Fig.4.5, in conjunction with contribution to shear force by the boundary columns, the wing walls and the central wall panels.

Q_p were increased with the increase of compressive concrete strength. Then, the contribution to shear

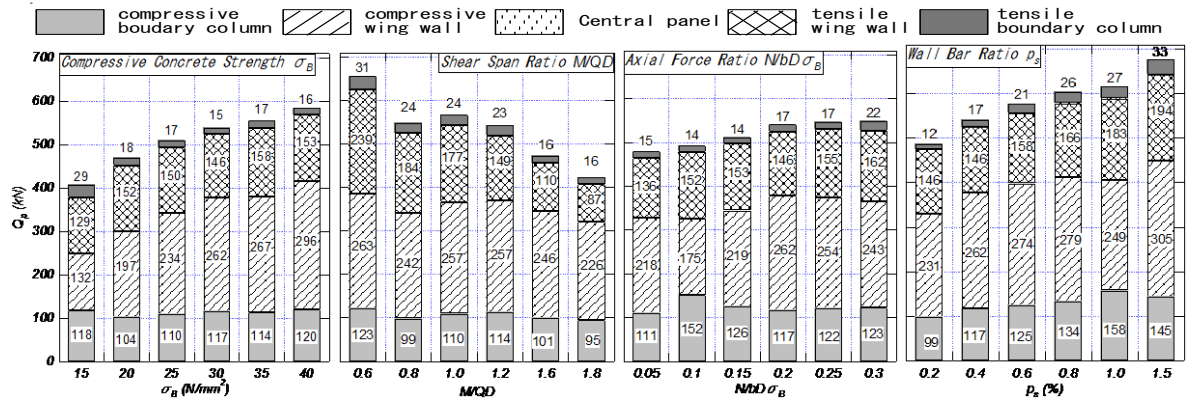


Figure 4.5. Q_p - influencing factors relationships (Specimen WO1)

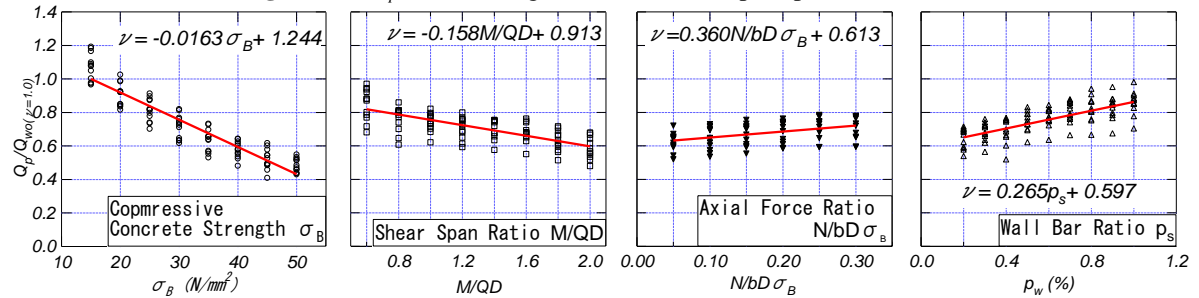


Figure 4.6. $Q_p/Q_{wo(v=1.0)}$ – influencing factors relationships

force by the wing wall under compression was especially increased. It is speculated that the transmissive shear of compressive struts were increased with the increase of internal stress in the compressive struts. In the relationship between Q_p and axial force ratios shows that the calculated shear strengths by the parametrical studies increased slightly proportional to the axial force ratios. In the relationship between Q_p and wall steel bar ratios, it was also showed the same tendency. On the other hand, in the relationship between Q_p and shear span ratios, Q_p decreased with the increase of shear span ratio. Especially, the decrease of the contribution to shear force by the tensile wing wall became noticeable. The reason why the compressive stress in the tensile wing wall decreased is because the overturning moment at bottom of shear wall was increased through the increase of shear span ratio.

4.3.3. Examination of Effective Factor for Compressive Strength of Concrete

From the analytical results, it was shown that the shear strength of RC shear walls varied with the increase or decrease of influencing factors. In this section, Effective factor for compressive strength of concrete ν was examined to reflect these tendencies in proposed model.

The calculated shear strengths by the parametrical studies for compressive strength of concrete, shear span ratio, axial force ratio and wall bar ratio are plotted in Fig.4.6. The vertical axis shows the ratios of the shear strengths evaluated by the parametrical analysis, Q_p , to those calculated by Eqn.4.1 and Eqn.4.2 with the effective factor for compressive strength of concrete ν of 1.0, $Q_{wo} (v=1.0)$, while horizontal axis are the influencing parameters such as compressive strength of concrete, shear span ratio, axial force ratio and steel bar ratio. The shear strength of RC shear walls with openings, Q_{wo} , is the sum of calculations given by Eqn.4.1 in the boundary columns, wing walls and central wall panels as shown in Eqn.4.2 in which the boundary columns are assumed as explained in Chapter .4.2.

$$Q_{wo} = \sum_{i=1}^{n+1} Q_{wi} \quad (4.2)$$

where, n: number of openings

Fig.4.6 shows a regression analysis between Q_p/Q_{wo} and each influencing factor respectively. From this analysis, the following equations were obtained.

$$v = -0.0163\sigma_B + 1.244 \quad (4.3)$$

$$v = -0.158\frac{M}{QD} + 0.913 \quad (4.4)$$

$$v = 0.360\frac{N}{bD\sigma_B} + 0.613 \quad (4.5)$$

$$v = 0.265p_s + 0.597 \quad (4.6)$$

$$v = x_1 \cdot \sigma_B + x_2 \cdot \frac{M}{QD} + x_3 \cdot \frac{N}{bD\sigma_B} + x_4 \cdot p_s + x_5 \quad (4.7)$$

Assuming Eqn.4.7 from Eqn.4.3, Eqn.4.4, Eqn.4.5, and Eqn.4.6, it was developed unknown letter $x_1 \sim x_5$ from the system of linear equations as shown in following equations.

$$v = (x_1 + 0.0163) \cdot \sigma_B + x_2 \cdot \frac{M}{QD} + x_3 \cdot \frac{N}{bD\sigma_B} + x_4 \cdot p_s + x_5 - 1.244 = 0 \quad (4.8)$$

$$v = x_1 \cdot \sigma_B + (x_2 + 0.158) \cdot \frac{M}{QD} + x_3 \cdot \frac{N}{bD\sigma_B} + x_4 \cdot p_s + x_5 - 0.913 = 0 \quad (4.9)$$

$$v = x_1 \cdot \sigma_B + x_2 \cdot \frac{M}{QD} + (x_3 - 0.360) \cdot \frac{N}{bD\sigma_B} + x_4 \cdot p_s + x_5 - 0.613 = 0 \quad (4.10)$$

$$v = x_1 \cdot \sigma_B + x_2 \cdot \frac{M}{QD} + x_3 \cdot \frac{N}{bD\sigma_B} + (x_4 - 0.265) \cdot p_s + x_5 - 0.597 = 0 \quad (4.11)$$

Solving the system of equations between Eqn.4.8, Eqn.4.9, Eqn.4.10 and Eqn.4.11, the equation of effective factor for compressive strength of concrete is shown in Eq.4.12.

$$v = -0.016\sigma_B - 0.16\frac{M}{QD} + 0.36\frac{N}{bD\sigma_B} + 0.27 \cdot p_s + 1.23 \quad (4.12)$$

4.4. Validity of Proposed Model

The procedure for the estimation of the shear strength of RC shear walls with multi-openings using proposed model is described below.

- 1) The shear strength in the boundary columns, wing walls and central wall panels are calculated by Eqn.4.1. Where, the effective factor for compressive strength of concrete v is given by Eqn.4.12.
- 2) The wing walls which have a boundary column in compression are assumed as explained in Chapter. 4.2
- 3) Shear strength of RC shear walls with openings is the sum of the calculations given by Eqn.4.1 in the boundary columns, wing walls and central wall panels

The relationships between the experimental shear strength and the calculated ones by proposed model are shown in Fig.4.7. The ratios of the shear strength by the experimental results to those calculated by the proposed model were approximately ranging from 0.8 to 1.2. Therefore, it is clarified that the shear strength of RC shear walls with multi-openings can be evaluated by the proposed simplified model. Also, using Eqn.4.12, it is possible to take into consideration the effect of the variation of influencing parameters on the shear strength of RC shear walls.

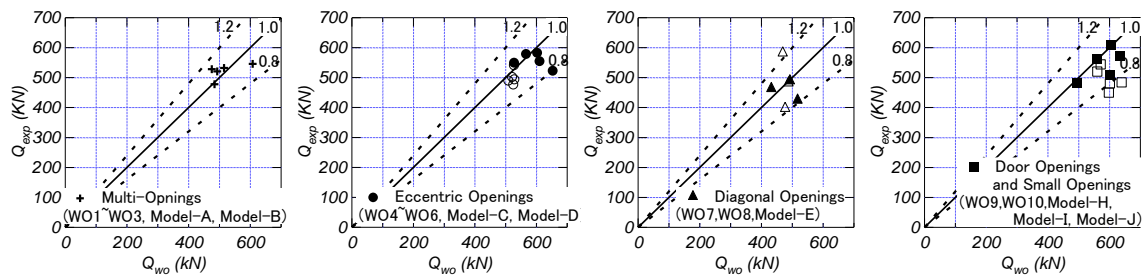


Figure 4.7. $Q_{exp} - Q_{wd}$ relationships

5. CONCLUSIONS

In this paper, parametrical analyses based on two dimensional non-linear FEM analysis were conducted for the shear walls with several opening layouts. From the analytical results, a simplified model to estimate the shear strength of RC shear walls with multi-openings was constructed. The following conclusions can be drawn.

- 1) The analytical results showed that the compressive diagonal struts transferring the shear stress are formed in each wall element and the shapes depend on the wall panel length.
- 2) The contribution to shear force of each wall element increase with the increase of the depth of wall similarly to compressive struts.
- 3) The boundary columns in tension contribute only about 10% or less to the maximum shear strength.
- 4) The shear strength of RC shear walls with multi-openings can be evaluated by the proposed model.
- 5) Using Egn.4.12, it is possible to take into consideration the effect of the variation of influencing parameters on the shear strength of RC shear walls with multi-openings.

AKNOWLEDGEMENT

This work was supported by Grant-in-Aid for Japan Society for the Promotion of Science (JSPS) Fellows.

REFERENCES

- Architectural Institute of Japan. (2010). AIJ Standards for Structural Calculation of steel Reinforced Concrete Structures. (In Japanese)
- Sakurai, M., Kuramoto, H., T., Matsui, and Akita, T. (2008). Seismic Performance of RC Shear Walls with Multi-openings, *Proceedings of 14th World Conference on Earthquake Engineering*, Paper-ID12-03-0071.
- Sakurai, M., T., Matsui, and Kuramoto, H. (2009). FEM Simulation for RC Shear Walls with Multi-Openings, *Proceedings of The 11th Taiwan-Korea-Japan Joint Seminar on Earthquake Engineering for Building Structures*, 121-129
- Sakurai, M., T., Matsui, and Kuramoto, H. (2010). Effect of Opening Arrangement on Shear Failure Mode of RC Shear Walls with Multi-Openings, *Proceedings of The 12th Taiwan-Korea-Japan Joint Seminar on Earthquake Engineering for Building Structures*, 247-254
- Architectural Institute Japan. (1999). Design Guidelines for Earthquake Reinforced Concrete Buildings Based on inelastic displacement concept. (In Japanese)
- Naganuma, K., Yonezawa, K., Kurimoto, O. and Eto, H. (2004). Simulation of nonlinear dynamic response of reinforced concrete scaled model using three-dimensional finite element method, *Proceedings of 13th World Conference on Earthquake Engineering*, **No.586**, paper.
- ITOCHU Techno-Solutions Corporation (2004). FINAL/99 HELP (In Japanese)
- Naganuma, K., Kurimoto, O. and Eto, H. (2001). Finite Element Analysis of Reinforced Concrete Walls Subjected to Reversed Cyclic and Dynamic Loads, *Journal of structural and construction engineering*, **No.544**, 125-132. (In Japanese)
- Kupfer, B., and Gerstle, H. et al. (1973). Behavior of Concrete under Biaxial Stress, *Journal of the engineering mechanics division*, 853-866
- Naganuma, K. (1991). Nonlinear Analytical Model for Reinforced Concrete Panels under In-Plane Stresses, *Journal of structural and construction engineering*, **No.421**, 39-48 (In Japanese).
- Yamaguchi, T. and Naganuma, K. (1990). Experimental Study on Mechanical Characteristics of Reinforced Concrete Panels Subjected to In-Plane Shear Force, *Journal of structural and construction engineering*, **No.419**, 77-86. (In Japanese)
- Naganuma, K. and Ohkubo, M. (2000). An Analytical Model for Reinforced Concrete Panels under Cyclic stresses, *Journal of structural and construction engineering*, **No.536**, 135-142. (In Japanese)
- Ciampi, V. et al. (1982). Analytical Model for concrete anchorages of reinforcing bars under generalized excitations, *Earthquake Engineering Research Center*, **Report No.EERC-82/83**, paper.